RSC Advances

ROYAL SOCIETY OF CHEMISTRY

www.rsc.org/advances

Fabrication of dendrimer-modified boronate affinity material for online selective enrichment of *cis*-diol-containing compounds and its application in determination of nucleosides in urine

Li Gao, Jin Du, Chaozhan Wang, Yinmao Wei*

Key Laboratory of Synthetic and Natural Function Molecule Chemistry of Ministry of Education, College of Chemistry and Materials Science, Northwest University, Xi'an 710069, China

Tel: +86-29-88302604;
Fax: +86-29-88302604;
E-mail: ymwei@nwu.edu.cn;

Abstract

Boronate adsorbents have been widely used in the extraction of *cis*-diol-containing molecules, but most do not have efficient capacity due to limited binding sites on their surface. In this work, a high binding capacity dendrimer-modified boronate affinity material (SiO_2@dBA) was synthesized via introducing tris(2-aminoethyl)amine as branching points and using poly(amidoamine) as the main dendrimeric scaffold before modification by boronate groups. The high density of amino groups on the dendrimer supplied a large number of binding sites for modifying boronate groups. Thus the adsorption capacity (676.8 μmol/g for catechol, 771.3 μmol/g for dopamine, 770.0 μmol/g for adrenaline) of SiO_2@dBA was greatly improved. Moreover, when coupled with large-volume injection and online column-switching solid phase extraction, SiO_2@dBA was able to capture *cis*-diols from 10000-fold interference and enrichment factors reached up to 497~514, which was 8- to 10-fold higher than those of analogous non-dendrimer materials. Especially, the proposed method exhibited a striking low limit of detection, 0.24 ng/mL for cytidine, 0.52 ng/mL for uridine, 0.37 ng/mL for guanosine, 0.67 ng/mL for adenosine. Finally, the method was successfully applied to online determination of trace nucleosides in healthy human urine. In conclusion, the prepared adsorbent has potential to effectively enrich a large scale of trace *cis*-diol substances in real samples.

Keywords: dendrimer-modification, boroate affinity chromatography, binding capacity, *cis*-diol containing compounds, nucleosides

1. INTRODUCTION

Cis-diol-containing biomolecules such as gylcoproteins, glycopeptides, carbohydrates, catechols and nucleosides play essential roles in many biological processes and are significant in disease diagnosis [1-5]. A common feature of most *cis*-diol-containing biomolecules is that in real samples they usually exist in very low abundance along with abundant interfering components [6], especially in the early phase of cancer and other degenerative diseases, causing considerable difficulty in analysis. Therefore, sample pretreatment including specific capture and effective enrichment process is necessary prior to instrumental analysis.

The applied techniques for isolation and enrichment of *cis*-diol-containing compounds mainly include lectins [7], hydrazide [8], antibodies [9], hydrophilic interaction liquid chromatography [10-12] and boronate affinity chromatography [13-21]. Unfortunately, lectins and antibodies are not only difficult to prepare but also are unstable. Although hydrazide chemistry is an efficient method, the reaction step is time-consuming and is easy to cause the change in the structure of the target molecules. As for hydrophilic interaction liquid chromatography, the selectivity is poor. Compared with the above approaches, boronate affinity chromatography gains increasing attention in recent years due to its significant advantages such as high specificity, easy-to-manipulate through pH switch, low cost and compatibility with mass spectrometry (MS) [13, 22-24].

Boronate affinity material is well known as a powerful sorbent for the selective isolation and enrichment of *cis*-diol-containing compounds. The principle relies on reversible covalent complex formation/dissociation between boronic acids and *cis*-diols in an alkaline/acidic aqueous solution. Generally, in the evaluation of boronate affinity materials, selectivity and binding capacity are two main characteristics [25]. That is to say, materials with strong boronate affinity ability at lower pH condition and high-density boronate affinity groups are essential. To improve selectivity, several strategies have been investigated for synthesizing various aromatic boronic acids or their derivatives with a lower pKa value [26-28]. On the other hand, to improve binding capacity, the density of functional groups on the surface of boronate affinity material is required to increase. Based on the styles of material surface modification, boronate affinity materials can be classified into three types, including small molecule-modification, polymer-modification

and dendrimer-modification. However, conventional boronate affinity materials with small molecule-modification are not satisfactory due to the limited binding sites on the material surface, which affect the enrichment efficiency of *cis*-diol molecules [29, 30].

Recently, the polymer-modification of boronate affinity materials has been developed to improve binding capacity. Li et al. grafted polyethyleneimine onto the surface of Fe_3O_4@SiO_2 before modification by boronate groups. Due to a high density of amino groups, polyethyleneimine polymer can supply a large number of active binding sites, which produced an adsorbent that exhibited a much higher adsorption capacity for *cis*-diol-containing compounds compared with the analogous materials [31]. Ye et al. grafted a fluorescent boronic acid polymer onto a silica surface via surface-initiated atom transfer radical polymerization (SI-ATRP). The obtained composite material contains repeating boronic acid units (polymer brushes) on surface and shows favorable binding capability [32]. And recently, our group synthesized an adsorbent with high binding capacity of 513.6 μmol/g for catechol and 736.8 μmol/g for fructose via the combination SI-ATRP and end-capped technology. Because of high binding capacity, only 2.0 mg of adsorbent could still eliminate interferences and yielded a recovery range of 85.6～101.1% in the enrichment of three *cis*-diol drugs from plasma [33].

The common feature of these polymer-modified boronate materials is that they contain a large number of active binding sites for grafting abundant functional ligands, and the obtained binding densities of functional ligands are much larger than those of small molecule-modification. Unfortunately, these polymer-modified materials still have their own limitations. Xue et al. demonstrated that because of steric hindrance, a large amount of unreacted amino groups on polyethyleneimine may generate strong electrostatic interaction with the analytes, thus affect the boronate affinity adsorption [34]. As for SI-ATRP reaction, it must be carried out under strictly anaerobic conditions and heavy metal catalysis, giving rise to pollution.

In contrast, dendrimers display obviously many excellent advantages, such as good solubility and extremely high density of functional groups, and are good candidates for single site catalyst, efficient adsorbents and sensors [35]. Wang et al. prepared magnetic molecularly imprinted adsorbent by using the dendronized SiO_2-coated magnetic nanoparticles as the supporter, aiming to avoid residual template leakage and to increase

the imprinting efficiency. The resulting magnetic molecularly imprinted adsorbent showed high adsorption capacity, fast binding kinetics and good selectivity for trace estrogens [36]. Yoo et al. fabricated a functionalized membrane via grafting hyperbranched poly(amidoamine) (PAMAM) onto the surface of poly(tetrafluoroethylene). The grafted membranes successfully adsorbed Cu^{2+} ions from aqueous solution with an adsorption capacity of 1.42 g/m^2 and demonstrated a highly efficient and reusable material for the removal of heavy metal ions [37]. Liu et al. synthesized the dendrimer-modified boronic acid-functionalized magnetic nanoparticles, which exhibited high binding capacity and fast binding/desorption speed towards *cis*-diol-containing compounds [38]. Although the advantages of dendrimer-modified materials have been demonstrated, it is still necessary to explore new applications of this type of modification in boronate affinity chromatography.

In this work, a dendrimer-modified boronate affinity material (SiO_2@dBA) with high capacity was prepared via introducing tris(2-aminoethyl)amine as branching points and anchoring PAMAM as the main dendrimeric scaffold, followed by reacting SiO_2@PAMAM with 4-formylphenylboronic acid (4-foPBA). Considering that online solid phase extraction (SPE) can enhance the analytical efficiency and automation, we employed the SiO_2@dBA for column-switching SPE coupled with high performance liquid chromatography (HPLC) with large-volume injection to facilitate the determination process of *cis*-diol-containing compounds. The selectivity and binding capacity were evaluated. Finally, SiO_2@dBA was applied to selectively enrich and analyze four nucleosides (uridine, adenosine, cytidine, guanosine) in healthy human urine.

2. EXPERIMENTAL SECTION

2.1. Chemicals and Materials.

Spherical silica (5 μm particle size; 70 Å pore size; 440 m^2/g surface area) was purchased from LanZhou Insititute of Chemical Physics, Chinese Academy of Sciences (Lanzhou, China); tris(2-aminoethyl)amine was purchased from Ourchem biological technology Co. Ltd (Shanghai, China); 4-(chloromethyl) phenyltrimethoxysilane (4-CPTS) was purchased from Alfa Aesar Chemical Reagent Co. Ltd (Qingdao, China); dopamine hydrochloride, sodium cyanoborohydride, guanosine, adenosine were purchased from Aladdin Chemical Reagent Co. Ltd (Shanghai, China). 4-foPBA, cytidine,

uridine were purchased from J&K Chemical Reagent Co. Ltd (Beijing, China); adrenaline was purchased from Sigma-Aldrich Fluka biochemical reagent Co. Ltd (America). Other regents were all of analytical grade.

2.2. Synthesis of SiO_2@dBA stationary phase

2.2.1. Immobilization of tris(2-aminoethyl) amine onto silica

The preparation procedure is illustrated in Fig.1. Silica-Cl was synthesized by the reported method [33]. Under nitrogen, silica (5.0 g) was dispersed in dried toluene (100 mL) and then 4-CPTS (2.2 mL, 10 mmol) was added; the reaction mixture was then stirred at 110℃ for 12 h. The Silica-Cl was filtered out, washed with toluene and methanol, and dried at 50 ℃ for 4 h under vacuum. Then, Silica-Cl (2.0 g), tetrahydrofuran (40 mL), tris(2-aminoethyl)amine (0.8 mL, 5 mmol), pyridine (0.1 mL) were added into a flask and the reaction mixture was stirred at 65 ℃ for 24 h. The resulting SiO_2@NH_2 was filtered out, washed with tetrahydrofuran, methanol, acetone in sequence and dried at 50℃ for 4 h under vacuum.

2.2.2. Surface modification with PAMAM dendrimer

SiO_2@PAMAM was synthesized by the reported method [39]. 2.0 g of the SiO_2@NH_2 was dispersed in 48 mL of sodium methylate, and then 12 mL of methylacrylate was added under stirring at room temperature for 7 h, immersing in an ultrasonic water bath. After reacting, the silica was collected and rinsed with methanol five times by vacuum filtration. Subsequently, 40 mL of 50% ethylenediamine (EDA) -methanol solution (v/v) was added into the silica, and the suspension was immersed in an ultrasonic water bath under stirring at room temperature for 3 h. The obtained SiO_2@PAMAM was then washed with methanol, acetone and then dried at 45℃ for 6 h under vacuum.

2.2.3. Surface modification with 4-foPBA

2.0 g of the obtained SiO_2@PAMAM was re-dispersed in 30 mL of dry methanol under ultrasonication. To the mixture, 4-foPBA (2.0 g, 13.4 mmol) and sodium cyanoborohydride (1.7 g, 27.0 mmol) were added under stirring. After stirring at room temperature for 72 h, the products were washed with 5% $NaHCO_3$, 5% NaCl and distilled water. The products were dried at 40℃ under vacuum to obtain SiO_2@dBA.

2.3. Characterization of the SiO_2@ dBA

Transmission electron microscopy (TEM) was performed on a FEI, Tecnai G2F20 S-TWIN microscope. Specific surface area and pore size analyzer (Tristar II 3020, Micromeritics Instrument Corporation, USA) was used to measure the BET surface area, the cumulative pore volume and the average pore diameter of the adsorbent. The X-ray photoelectron spectroscopy (XPS) analysis (K-Alpha, the rmo Fisher Scientific) was carried out to determine the chemical states. Fourier transform spectrometer (TENSOR 27, Bruker, Germany) was used to determine the surface composition of the adsorbent. Thermal gravimetric analyses (TGA) were performed in an air stream using a Perkin-Elmer STA 6000 thermal analyzer at a heating rate of 10℃／ min.

2.4. Online extraction procedures

1.0 g of the obtained SiO_2@dBA was dispersed into pure methanol and packed into a 50 mm×4.6 mm I.D. stainless column by multipacking (GY-50B, made in China) at 35 MPa.

A column-switching SPE/HPLC system was illustrated in Fig. 2. Briefly, the online extraction includes several steps. (a) Precondition. The 6-port switching valve was set to position 1. The boronate affinity SPE column and the C18 column (5 μm, 4.6 mm×150 mm) were equilibrated with mobile phase A (5 mM ammonium formate/acetonitrile, pH = 2.5, v/v = 98:2) at a flow rate of 1.0 mL/min. Then the 6-port switching valve was switched to position 2, only the boronate affinity SPE column was equilibrated with mobile phase B (50 mM ammonium chloride, pH = 8.5). (b) Extraction. The 6-port switching valve was kept in position 2. After 10 mL sample solution was injected, mobile phase B was pumped to flow through the boronate affinity column at a flow rate of 1.0 mL/min for 5 min. (c) Desorption. After extraction, the 6-port switching valve was switched to position 1 again, and at the same time 100% mobile B was switched to 100% mobile A for desorption and analysis.

Without column-switching system, the 6-port switching valve was maintained at position 1, 20 μL of the sample was directly injected with mobile phase A (5mM ammonium formate/acetonitrile, pH = 2.5, v/v = 98:2) at a flow rate of 1.0 mL/min.

2.5. Chromatographic conditions

All chromatographic experiments were performed on a Shimadzu HPLC system

(Kyoto, Japan), consisting of two LC-10ATvp pumps, a SCL-10A system controller, a UV–vis detector and a CLASS VP 5.03 chromatography workstation. The chromatographic separation was performed on a VP-ODS column (4.6 mm × 150 mm) at room temperature. The mobile phase was filtered through a 0.45 μm Nylon membrane and degassed ultrasonically prior to use.

For the detection of nucleosides, the UV wavelength was set at 260 nm. While for catechol, quinol, salbutamol, dopamine, adrenaline and isoprenaline, the wavelength was set at 280 nm.

2.6. Sample pretreatment

Urine samples were collected from one healthy volunteer from our laboratory, added with sodium metabisulfite (1 mg/mL) and stored in refrigerator. Then the urine sample was diluted with pure water (1:4) and filtered through a 0.45 μm membrane prior to online analysis.

3. RESULTS AND DISCUSSION

3.1. Preparation of the SiO_2@dBA column

As for traditional PAMAM, G1 generation is often fabricated through two-step reactions: half generation dendrimers terminate with carboxylate ester group, then full generation dendrimers terminate with amino groups [40]. In this work, G1 generation was directly synthesized by one-step reaction via introducing tris(2-aminoethyl)amine as branching points, as shown in Fig.1. Compared with the reported method [40], the present method simplified the process of dendrimer-modification. In addition, abundant functional sites of the boronic acid groups provided the possibility to enhance the binding strength and binding capacity significantly.

For comparison, a non-dendrimer-modified boronate affinity column was also prepared using EDA as a substitute of tris(2-aminoethyl)amine and followed by directly grafting 4-foPBA on SiO_2@EDA, and the as-prepared adsorbent was marked as SiO_2@BA. In this part, the enrichment factor (EF) was determined via online column-switching SPE-HPLC for the determination of nucleosides on both columns. EF is known as the ratio of the analyte concentration in the eluent (C_{elu}) to the initial concentration of the analyte (C_o) within the sample.

$$EF = \frac{C_{elu}}{C_o} \qquad (1)$$

As shown in Fig. 3, the EFs of SiO_2@dBA column toward four nucleosides exhibited 26～51 folds higher than that of non-dendrimer-modified column. The impressive better extraction ability should be attributed to the highly branched PAMAM dendrimers, which increased the density of boronic acid ligand on the surface of the adsorbent. Furthermore, different EFs between the SiO_2@dBA column and SiO_2@BA column can prove the successful dendrimer-modification.

3.2. Characterization of SiO_2@dBA

Representative TEM images of bare silica and SiO_2@dBA were provided in Fig. S1. There was no obvious difference between the TEM images of bare silica and SiO_2@dBA, suggesting that dendrimer do not appear to block the mesopore.

In addition, characterization of the pore structure of SiO_2@dBA was also performed by nitrogen adsorption-desorption measurement (Fig. 4A). According to the N_2 sorption analysis, the BET surface area of SiO_2@dBA was 194 m^2/g, BJH desorption cumulative volume of pores was 0.34 m^3/g and the pore size was 6.8nm. Compared to that of the bare silica (Table S1), the S_{BET} and pore volume of SiO_2@dBA decreased by about 50%, whereas the pore size decreased by 3%. The behavior of the structural properties demonstrated that the dendrimer grew inside the pore channels, which was consistent with the reported research [41].

XPS (Fig. 4B) indicated the strength of N 1s peak at 399.8 eV for SiO_2@PAMAM was stronger than that for SiO_2@NH_2, and the calculated N content increased from 2.27% for SiO_2@NH_2 to 4.30% for SiO_2@PAMAM (Table 1), indicating that the density of amino groups was increased via dendrimer-modification. Higher content of N provided a larger number of active binding sites, and also improved the hydrophilicity of the material. The appearance of a B1s peak at 191.4 eV on SiO_2@dBA exhibited the successful attachment of boronic acid groups onto the SiO_2@PAMAM.

According to the boron content, the density of the grafted 4-foPBA on the silica ($\mu mol/m^2$) was calculated by the following equation [42]:

$$\text{Gafted } 4-\text{foPBA} = \frac{\%B\ (10^6)}{\%B_{(calcd.)} \times \left(1 - \frac{\%B}{\%B_{P(calcd.)}}\right) \times M \times S} \qquad (2)$$

Where %B is the boron percent determined by XPS, $\%B_{(calcd.)}$ is the calculated weight percent of boron in 4-foPBA, M is the formula weight of 4-foPBA and S is the

specific surface area of the prepared silica in a unit of m^2/g.

By combination of the B content and the specific surface area, the surface coverage of 4-foPBA on the silica was calculated to be 3.6 μmol/m^2. And according to the coverage, the N content of the obtained SiO_2@dBA was calculated to be 3.57 %, which was close to the value of 3.69 % determined by XPS. So there were few residual amine groups on the surface of SiO_2@dBA.

The Fourier transform infrared (FT-IR) spectrum shown in Fig. 4C also indicated the successful modification in different stages. The broad absorption band at 3434 cm^{-1} corresponded to the stretching vibration of N–H/O-H bonds. For c and d, the band observed at 1647 cm^{-1} was indicative of C=O stretching while that at 1518 cm^{-1} could be attributed to the coupling of C–N stretching vibration and N–H bending vibration, which indicated the successful attachment of PAMAM onto the SiO_2@NH_2. The peaks at 2850 cm^{-1} and 2930cm^{-1} were characteristic of the C-H/CH_2 stretching vibration bands. Generally, the SiO_2@dBA had similar absorption peaks with the SiO_2@PAMAM expect for the typical absorption peak of B-O at 1342 cm^{-1}. The results verified the presence of boric acid groups on the surface of SiO_2@dBA.

Furthermore, the indication of the coating formation on the silica surface can be obtained from TGA measurement. As shown in Fig. 4D, the weight loss profile for bare silica, SiO_2@NH_2, SiO_2@PAMAM and SiO_2@dBA exhibited two different stages within the range of 25℃ to 500℃. Below 200℃, all of them presented a weight loss profile for the release of water or physically adsorbed solvent. And there was an obvious weight loss of 3.8% from 200℃ to 400℃ for SiO_2@NH_2, and 5.6% and 8.1% for SiO_2@PAMAM and SiO_2@dBA from 200℃ to 500℃, respectively. The increased weight loss suggested that tris(2-aminoethyl)amine, the PAMAM dendrimer and 4-foPBA were successfully grafted on the silica.·

3.3. Selectivity

The selectivity of the SiO_2@dBA was evaluated by extracting *cis*-diols isoprenaline and salbutamol from a mixed solution containing non-*cis*-diols quinol and 2'-deoxyadenosine as interferences. The mixture was extracted and analyzed by online column-switching SPE-HPLC system. The total amount of the *cis*-diols did not exceed

the maximum binding capacity of SiO_2@dBA. The molar ratio of interferences to targets was increased from 1:1 to 10000:1. Such an experiment design was able to vary the competition adsorption between *cis*-diols and non-*cis*-diols, favoring the reflection of the specific binding.

It can be seen from Fig. 5 that isoprenaline and salbutamol could be captured as the molar ratio of interferences and targets increased from 1:1 to 100:1. Even if the molar ratios went up to 10000:1, they were all distinguished from the background after the online SPE procedure. Therefore, the prepared SiO_2@dBA exhibited specific selectivity towards *cis*-diols over non-*cis*-diol analogs. Moreover, the molar ratio was performed as the concentrations of interferences remained unchanged and the concentrations of the targets reduced gradually. When the concentration of isoprenaline and salbutamol was low to 10 ng/mL along with 10000 fold non-*cis*-diol interferences，their signals after online enrichment could still be detected with UV detection. The high sensitivity was ascribed to the high density of boronate affinity binding sites, which provided the possibility to achieve a low detection limit.

3.4. Binding/Loading capacity

Binding capacity is a crucial factor in affinity chromatography that determines the maximum amount of targets that an affinity column can capture. With offline SPE/HPLC system, the binding capacity of SiO_2@dBA was evaluated using static adsorption test with three small *cis*-diol compounds, catechol, dopamine and adrenaline. The binding isotherms of three *cis*-diol compounds were examined using different concentrations in the range of 0～1500 μg/mL. As shown in Fig. S2, the amounts of three *cis*-diol compounds bound to SiO_2@dBA increased with increasing concentrations until the binding saturation reached. The plateau of the curve corresponds to a maximum binding capacity of 676.8 μmol/g for catechol, 771.3 μmol/g for dopamine and 770.0 μmol/g for adrenaline, respectively. In contrast, the SiO_2@PAMAM did not show obvious binding. Clearly, the binding to SiO_2@dBA was contributed by the specific interaction between the *cis*-diols and the surface-modified boronic acid groups. And due to the higher active site density, the binding capacity of SiO_2@dBA is much higher than those of the reported extractive materials for *cis*-diol compounds capture [31, 32, 43-45]. While the binding capacity is similar with that of the polymer-modified material via ATRP and end-capped

technology reported by our group [33].

The sample loading capacity is a measure of the maximum amount of sample that can be injected into the column [46]. The "universal" overload curve provides a convenient approach to determine loading capacity. In this work, the overload curves were obtained on the HPLC system only using the SPE column with the same mobile phase as in the online SPE/HPLC system, and the injection volumes from low to high are blank, 5, 10, 20, 50, 100, 150, 200, 250 μL catechol solution (0.25 g/mL).

As shown in Fig. 6, with larger injection volume, the peak height showed an increasing trend, which was accompanied with the peak broadening at the same time. When the injection volume was less than 100 μL, the retention time of analyte basically remained unchanged. While the injection volume continued to increase, the retention time was shortened obviously and the peak shape was gradually changed to be asymmetrical. When the injection volume was more than 200 μL, the column loading capacity had exceeded the maximum value. In this case, the sample peak was significantly ahead of time, outflow with the solvent, even overlapped completely. Because once the column was overloaded, a part of the sample could not be reserved, which made the separation process much faster. Thus, it was concluded that the maximum injection volume of catechol was 150 μL, which corresponded to column loading capacity of 170 μmol/g.

3.5. Online column-switching SPE-HPLC for the determination of nucleosides

3.5.1. Method validation

An online column-switching SPE-HPLC system for the determination of four nucleosides was performed. As shown in Table 2, the linear range of the calibration curve was constructed at various concentration levels (1～50 ng/mL for cytidine and guanosine, 2～50 ng/mL for uridine and adenosine). Good linearities with squared regression coefficients (R^2) ranging from 0.9987 to 0.9998 were obtained. The repeatability was calculated by five parallel samples containing 10 ng/mL mixed standard solution, and the results showed satisfactory relative standard deviations (RSDs) of intra-day (2.7～7.9%) and inter-day (4.1 ～ 9.9%). The limits of detection (LODs) and the limits of quantification (LOQs) were calculated as the concentration corresponding to a signal 3 and 10 times the standard deviation of the baseline noise ratio, respectively. The LODs for four nucleosides were found to be 0.24～0.67 ng/mL. The LOQs were found to be

0.80～2.23 ng/mL.

There are two main aspects contributing to such low LODs. On the one hand, the packing material was synthesized by dendrimer-modification, which improved the density of functional groups greatly. On the other hand, the high enrichment performance should be attributed to the online column-switching SPE/HPLC with large-volume injection. To identify this idea, 20 μL of the sample was used under the same condition and no signal can be detected. However, when the injection volume increased to 10 mL, the signal of 1 ng/mL sample solution can still be detected with the online enrichment system.

Table 3 showed the comparison of the LODs of the proposed method with some other reported methods in the literature. Results demonstrated that the proposed method for the determination of four nucleosides in the present work showed a lower LODs than that of any other methods expect for the derivatization method. The LODs of the derivatization method was one order of magnitude lower than that of the proposed method, which was due to the introduction of the derivatization and high sensitive MS/MS as detector instead of UV detector.

3.5.2. Analysis of nucleosides in urine sample

In order to evaluate applicability of the proposed method for complicated samples, the extraction and determination of nucleosides (uridine, adenosine, cytidine, guanosine) was performed. As shown in Table 4, the urine samples were spiked at high (10 ng/mL), medium (5 ng/mL), low (1 ng/mL) three levels and analyzed using online column-switching SPE/HPLC with large-volume injection. Satisfactory recoveries at different spiking levels were in the range of 89% to 109% with RSDs of 1.6～5.3% for intra-day and 2.2～9.6% for inter-day. The detected concentrations of four nucleosides were 9.0 ng/mL for cytidine, 10.2 ng/mL for uridine, 13.5 ng/mL for guanosine and 16.8 ng/mL for adenosine, respectively, being lower than that found in the literature [47]. The possible reason may be that the concentrations of nucleosides in human urine are different by gathering from different volunteer at different time.

Fig.7 shows the chromatograms of 2 μg/mL nucleoside standard solution, urine sample, online enrichment urine sample without and with spiked with 5 ng/mL nucleosides. None of the nucleosides was detected in the blank urine sample without

enrichment due to a multitude of interferences originating from urine samples. By contrast, when the urine sample and the spiked urine sample were treated with online enrichment (Fig. 7c and Fig. 7d), only peaks of analytes were presented without interfering peaks. These results demonstrate the applicability of the proposed method for preconcentration and determination of nucleosides in real samples.

4. CONCLUSION

In this work, an effective adsorbent SiO_2@dBA was synthesized to capture *cis*-diol-containing compounds with online column-switching SPE-HPLC system. Several advantages were shown as follows: (1) By introducing tris(2-aminoethyl)amine, the reaction process of dendrimer-modification was simplified in the preparation of SiO_2@dBA. (2) Via dendrimer-modification, the density of amino groups was increased, which provided more binding sites and improved the hydrophilicity of the material. As a result, the prepared adsorbent showed excellent selectivity and remarkable binding capacity toward *cis*-diols compared with the reported adsorbent. (3) Owing to large-volume injection and online column-switching SPE-HPLC, predominant LODs and EFs made the prepared adsorbent serve as a promising alternative for the pretreatment of large scale biological samples. It is expected that this method can be exploited to widen its application for analysis of other *cis*-diol-containing biomarkers.

AUTHOR INFORMATION

Corresponding Author

*E-mail: ymwei@nwu.edu.cn (Y.M. Wei)

Acknowledgements

This work was supported by the National Natural Science Foundation of China (Nos. 21275115, 21475104 and 21575114)

References:

[1] Z. Yang, W.S. Hancock, J Chromatogr A, 2004, 1053, 79-88.
[2] Y.L. Wang, M.B. Liu, L.Q. Xie, C.Y. Fang, H.M. Xiong, H.J. Lu, Anal Chem, 2014, 86, 2057-2064.
[3] X.H. Pan, Y. Chen, P.X. Zhao, D.J. Li, Z. Liu, Angew Chem Int Ed Engl, 2015, 54, 6173-6176.
[4] M.M. Vivas, E.R. Gonzalo, D.G. Gómez, R.C. Martínez, J Chromatogr A, 2015, 1414，129-137.
[5] Y.B. Wu, J.H. Wu, Z.G. Shi, Y.Q. Feng, J Chromatogr B, 2009, 877, 1847-1855.
[6] B. Kammerer, A. Frickenschmidt, C.H. Gleiter, S. Laufer, H. Liebich, J Am Soc Mass Spectrom, 2005, 16, 940-947.
[7] B.F. Mann, A.K.P. Mann, S.E. Skrabalak, M.V. Novotny, Anal Chem, 2013, 85, 1905-1912.
[8] E.W. Song, R. Zhu, Z.T. Hammoud, Y.H. Mechref, J Proteome Res, 2014, 13, 4808-4820.
[9] B.C. Kim, M.K. Ju, A.D.C. Yu, P. Sommer, Anal Chem, 2009, 81, 2388-2393.
[10] O.H. Hernandez, R.L. Aguilar, J.E.Q. Lopez, M.L. Sanz, F.J. Moreno, J Proteomics, 2010, 10, 3699-3711.
[11] M.P.Y. Lam, S.O. Siu, E. Lau, X.L. Mao, H.Z. Sun, P.C.N. Chiu, W. S. B. Yeung, D. M. Cox, I. K. Chu, Anal Bioanal Chem, 2010, 398, 791-804.
[12] S. Mysling, G. Palmisano, P. Højrup, M.T. Andersen, Anal Chem, 2010, 82, 5598-5609.
[13] H.Y. Li, Z. Liu, Trac-trend Anal Chem, 2012, 37, 148-161.
[14] J. Tang, Y. Liu, P. Yin, G.P. Yao, G.Q. Yan, C.H. Deng, X.M. Zhang, J Proteomics, 2010, 10, 2000-2014.
[15] Z.J. Liu, K. Ullah, L.P. Su, F. Lv, Y.L. Deng, R.J. Dai, Y.J. Li, Y.K. Zhang, J Mater Chem, 2012, 22, 18753.
[16] Y.C. Liu, Y. Lu, Z. Liu, Chem Sci, 2012, 3, 1467.
[17] H.Y. Li, H.Y. Wang, Y.C. Liu, Z. Liu, Chem Commun, 2012, 48, 4115-4117.
[18] L.T. Liu, Y. Zhang, L. Zhang, G.Q. Yan, J. Yao, P.Y. Yang, H. J. Lu, Anal Chim Acta, 2012, 753, 64-72.
[19] S.T. Wang, D. Chen, J. Ding, B.F. Yuan, Y.Q. Feng, Chem-Eur J, 2013, 19, 606-612.
[20] Z.J. Bie, Y. Chen, H.Y. Li, R.H. Wu, Z. Liu, Anal Chim Acta, 2014, 834, 1-8.
[21] L. Liang, Z. Liu, Chem Commun, 2011, 47, 2255-2257.
[22] R. Tuytten, F. Lemière, W.V. Dongen, E. Witters, E.L. Esmans, R.P. Newton, E. Dudley, Anal Chem, 2008, 80, 1263-1271.
[23] J.G. He, Z. Liu, L.B. Ren, Y.C. Liu, P. Dou, K. Qian, H.Y. Chen, Talanta, 2010, 82, 270-276.
[24] Q.B. Zhang, N. Tang, J.W.C. Brock, H.M. Mottaz, J.M. Ames, J.W. Baynes, R.D. Smith, T. O. Metz, J Proteome Res, 2007, 6, 2323-2330.
[25] Q.J. Li, C.C. Lü, H.Y. Li, Y.C. Liu, H.Y. Wang, X. Wang, Z. Liu, J Chromatogr A, 2012, 1256, 114-120.
[26] L.B. Ren, Z. Liu, Y.C. Liu, P. Dou, H.Y. Chen, Angewandte Chemie, 2009, 121, 6832-6835.
[27] F.L. Li, X.J. Zhao, W.Z. Wang, G.W. Xu, Anal Chim Acta, 2006, 580, 181-187.
[28] J.G. He, Z. Liu, P. Dou, J. Liu, L.B. Ren, H.Y. Chen, Talanta, 2009, 79, 746-751.

[29] O. Çetinkaya, M.E. Duru, H. Çiçek, J Chromatogr B, 2012, 909, 51-60.
[30] P. Dou, L. Liang, J.G. He, Z. Liu, H.Y. Chen, J Chromatogr A, 2009, 1216, 7558-7563.
[31] H. Li, Y.H. Shan, L.Z. Qiao, A. Dou, X.Z. Shi, G.W. Xu, Anal Chem, 2013, 85, 11585-11592.
[32] Z.F. Xu, K.M.A. Uddin, T. Kamra, J. Schnadt, L. Ye, ACS Appl Mater Interfaces, 2014, 6, 1406-1414.
[33] W. Wang, M.F. He, C.Z. Wang, Y.M. Wei, Anal Chim Acta, 2015, 886, 66-74.
[34] Y. Xue, W.J. Shi, B.J. Zhu, X. Gu, Y. Wang, C. Yan, Talanta, 2015, 140, 1-9.
[35] A.E. Kadib, N. Katir, M. Bousmina, J.P. Majoral, New J Chem, 2012, 36, 241-255.
[36] S. Wang, R.Y. Wang, X.L. Wu, Y. Wang, C. Xue, J.H. Wu, J.L. Hong, J. Liu, X.M. Zhou, J Chromatogr B, 2012, 905, 105-112.
[37] H. Yoo, S.Y. Kwak, Journal of Membrane Science, 2013, 448, 125-134.
[38] H.Y. Wang, Z.J. Bie, C.C. Lü, Z. Liu, Chem Sci, 2013, 4, 4298-4303.
[39] B.F. Pan, F. Gao, H.C. Gu, J Colloid Interface Sci, 2005, 284, 1-6.
[40] E. Soršak, J.V. Valh, Š.K. Urekb, A. Lobnik, Analyst, 2014, 140, 976-989.
[41] J.P.K. Reynhardt, Y. Yang, A.H. Sayari, Alper, Adv Funct Mater, 2005, 15, 1641-1646.
[42] A. Mizutani, K. Nagase, A. Kikuchi, H. Kanazawa, Y. Akiyama, J. Kobayashi, M. Annaka, T. Okano, J Chromatogr A, 2010, 1217, 522-529.
[43] J. Du, M.F. He, X.M. Wang, H. Fan, Y.M. Wei, Biomed Chromatogr, 2015, 29, 312-320.
[44] D.J. Li, Y. Li, X.L. Li, Z.J. Bie, X.H. Pan, Q. Zhang, Z. Liu, J Chromatogr A, 2015, 1384, 88-96.
[45] N. Ozdemir, A. Cakir, B. Somturk, Colloids Surf A, 2014, 445, 40-47.
[46] J. Dai, P.W. Carr, D.V. McCalley, J Chromatogr A, 2009, 1216, 2474-2482.
[47] E.R. Gonzalo, D.G. Gomez, R.C. Martinez, J Chromatogr A, 2011, 1218, 9055-9063.
[48] M.L. Chen, S.S. Wei, B.F. Yuan, Y.Q. Feng, J Chromatogr A, 2012, 1228, 183-192.
[49] C.D. Laourdakis, E.F. Merino, A.P. Neilson, M.B. Cassera, J Chromatogr B, 2014, 967, 127-133.
[50] W. Struck, D. Siluk, A.Y. Mpanga, M. Markuszewski, R. Kaliszan, M.J. Markuszewski, J Chromatogr A, 2013, 1283, 122-131.
[51] L.B. Jeng, W.Y. Lo, W.Y. Hsu, W.D. Lin, C.T. Lin, C.C. Lai, F.J. Tsai, Rapid Commun Mass Sp, 2009, 23, 1543-1549.
[52] Y.Q. Jiang, Y.F. Ma, Anal Chem, 2009, 81, 6474-6480.
[53] E. Szymańska, M.J. Markuszewski, K. Bodzioch, R. Kaliszan, J Pharm Biomed Anal, 2007, 44, 1118-1126.
[54] S.F. Wang, X.P. Zhao, Y. Mao, Y.Y. Cheng, J Chromatogr A, 2007, 1147, 254-260.

Figure captions

Figure. 1. The route for synthesis of SiO_2@dBA.

Figure. 2. The schematic diagram of the column-switching SPE/HPLC system.

Figure. 3. Comparison of the EFs of SiO_2@dBA and SiO_2@BA towards four nucleosides.

Figure. 4. （A）Nitrogen adsorption-desorption isothermal plot with the inset showing the pore-size distribution of SiO_2@dBA; (B) XPS photograph; (C) FT-IR spectrogram; (D) TGA curves. (a) Pure silica; (b) SiO_2@NH_2; (c) SiO_2@PAMAM; (d) SiO_2@dBA.

Figure. 5. Chromatograms of the mixture of non-*cis*-diol and *cis*-diol-containing molecules analyzed without (a) and with (b) online SPE-HPLC column switching system with concentration ratios of 1:1, 10:1, 100:1, 1000:1, 10000:1. Peaks: 1, isoprenaline; 2, quinol; 3, 2'-deoxyadenosine; 4, salbutamol.

Figure. 6. Effect of loading amount of catechol on peak shape. Injection volume from bottom to top: blank, 5, 10, 20, 50, 100, 150, 200, 250 μL.

Figure. 7. Chromatograms of nucleosides. (a) 20 μL of 2 μg/mL mixed standard solution; (b) 20 μL of human urine; (c) Online enrichment of 10 mL of human urine; (d) Online enrichment of 10 mL of human urine spiked with 5.0 ng/mL. Peaks: 1, cytidine; 2, uridine; 3, guanosine; 4, adenosine.

508 **Table 1**

509 Elemental content obtained by XPS.

Sample/Element	Si2s/2p (%)	C1s (%)	O1s (%)	N1s (%)	B1s (%)
Bare silica	27.78	23.51	48.71	-	-
SiO_2@NH_2	16.10	48.14	33.48	2.27	-
SiO_2@PAMAM	17.39	44.95	33.36	4.30	-
SiO_2@dBA	12.43	57.19	26.03	3.69	0.66

510
511

Table 2

Method validation of nucleosides by online extraction with SiO_2@dBA SPE column.

Analyte	t_R (min)	Linear range (ng/mL)	R^2	LOD (ng/mL)	LOQ (ng/mL)	RSD (%, n=5)	
						Intra-day	inter-day
cytidine	14.8	1.0～50	0.9987	0.24	0.80	2.7	4.1
uridine	16.8	2.0～50	0.9997	0.52	1.73	7.8	8.9
guanosine	21.2	1.0～50	0.9996	0.37	1.23	5.4	6.6
adenosine	28.6	2.0～50	0.9998	0.67	2.23	7.9	9.9

Table 3

Comparison of the LODs in this work with the reported methods for the determination of nucleosides in urine.

Sample treatment	Analytical technique	LOD (ng/mL)				Reference
		Cytidine	Uridine	Guanosine	Adenosine	
Online SPE	LC-MS/MS	-	1.3	0.2	0.2	[47]
Online SPME	Capillary LC-UV	48	44	52	40	[48]
Derivatization	LC-MS/MS	0.037	0.16	0.026	0.034	[49]
PBA column	LC-MS/MS	80	180	-	80	[50]
SPE with Oasis MCX	LC-MS/MS	30	75	-	30	[51]
Affi-Gel 601	MEKC-UV	405	259	217	291	[52]
Affi-Gel 601	MEKC-UV	120	40	160	210	[53]
Affi-Gel 601	CE-MS	5.03	498	28.2	5.18	[54]
Online SPE-HPLC	LC-UV	0.24	0.52	0.37	0.67	This work

521 **Table 4**

522 Recoveries of four nucleosides in human urine.

Analyte	Conc. (ng/mL)	1 ng/mL			5 ng/mL			10 ng/mL		
		Recovery (%)	RSD(%)		Recovery (%)	RSD(%)		Recovery (%)	RSD(%)	
			Intra-day	Inter-day		Intra-day	Inter-day		Intra-day	Inter-day
cytidine	9	95	4.6	4.2	99	3.5	5	109	1.8	2.2
uridine	10.2	101	3.6	6.2	98	2.6	5.8	100	2.5	3.2
guanosine	13.5	103	5.3	7.3	104	1.6	3.2	98	3.0	3.9
adenosine	16.8	89	4.2	9.6	90	2.7	5	95	2.8	4.5

523

524

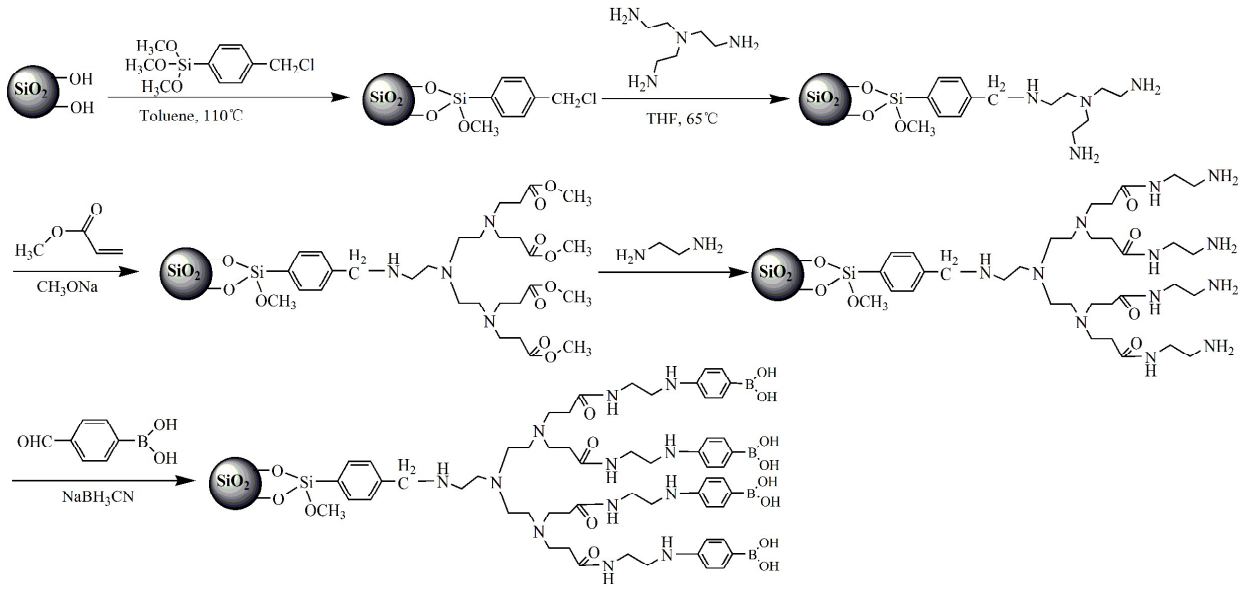

525
526

527 **Figure. 1.**

528

529

530

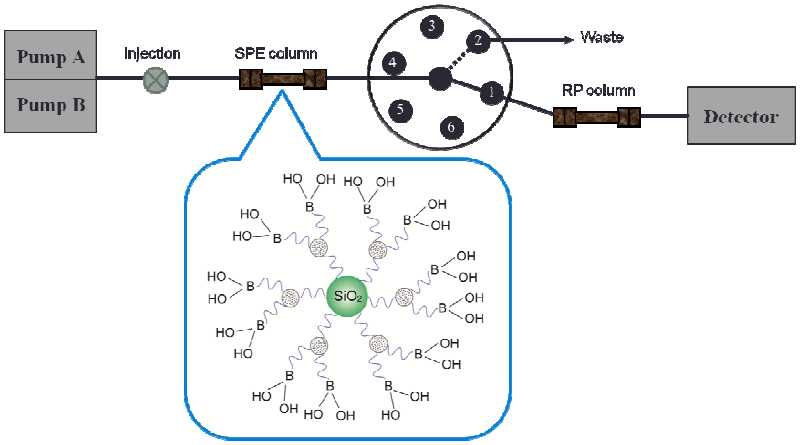

531

532 **Figure. 2.**

533

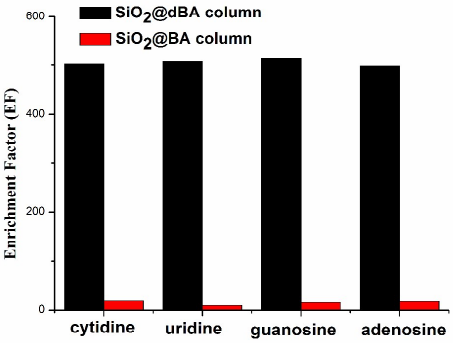

534

535 **Figure. 3.**

536

537

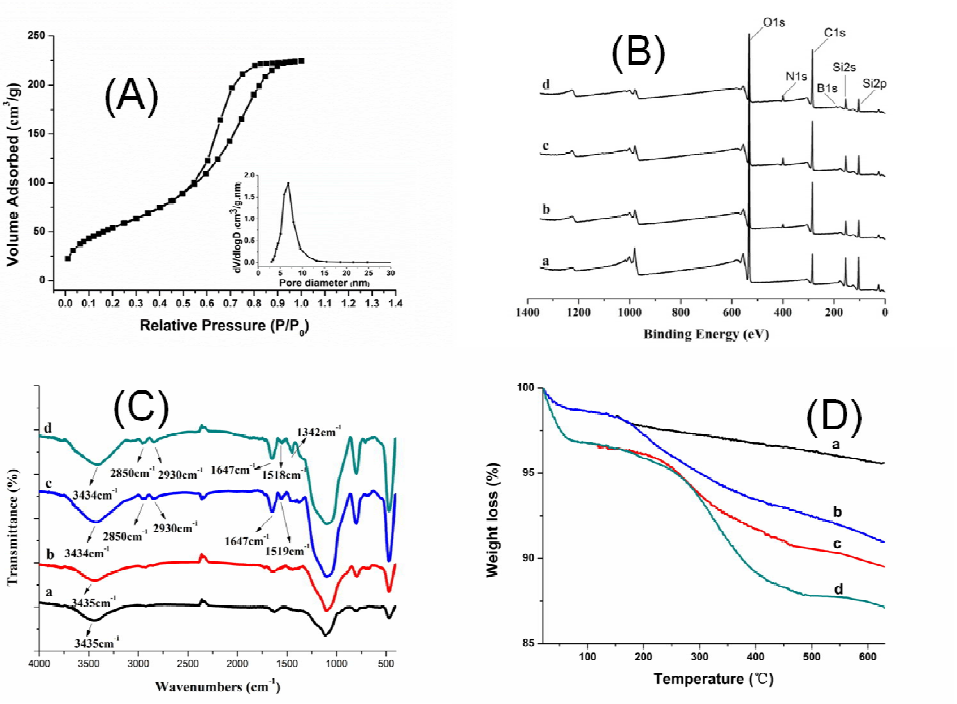

538

539 **Figure. 4.**

540

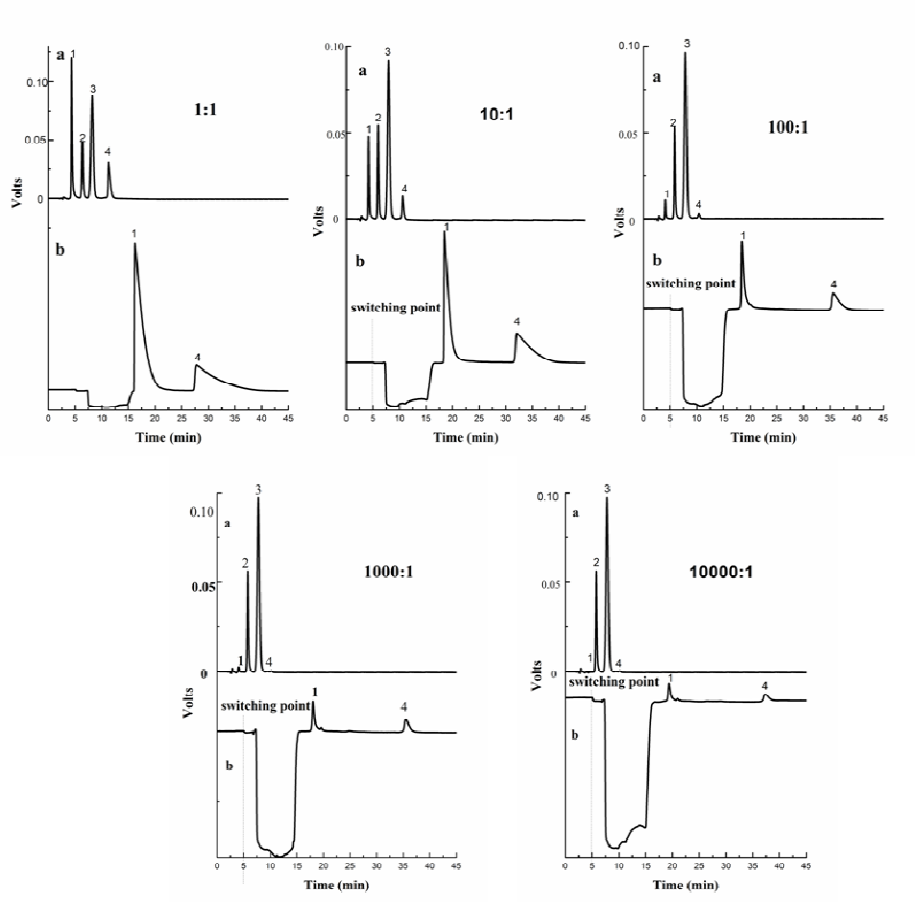

Figure. 5.

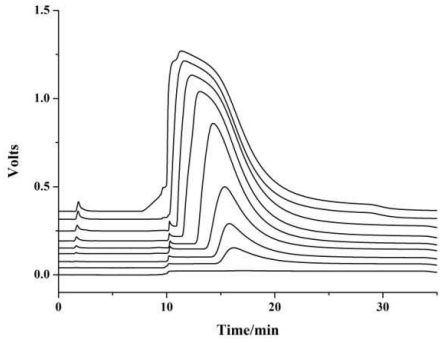

544

545 **Figure. 6.**

546

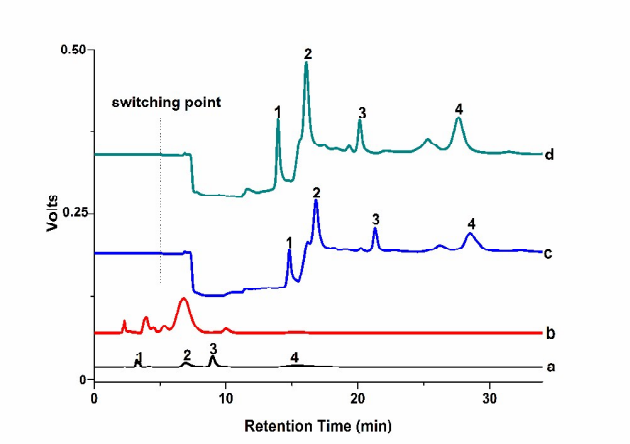

547

548 **Figure. 7.**

549

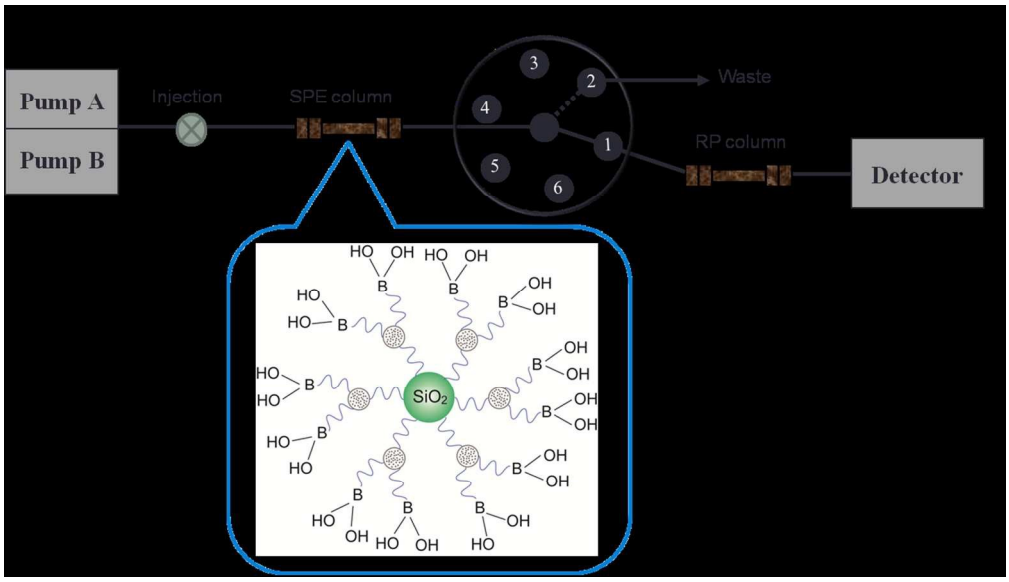

226x129mm (150 x 150 DPI)